Model of surface segregation driving forces and their coupling

Jérôme Creuze
LEMHE/ICMMO, Université Paris Sud, Bât. 410, F91405 Orsay Cedex, France

Isabelle Braems and Fabienne Berthier
CNRS, UMR 8182, F91405 Orsay Cedex, France

Christine Mottet and Guy Tréglia
CINaM-CNRS, UPR 2118, Campus de Luminy, Case 913, 13288 Marseille Cedex 9, France

Bernard Legrand
SRMP-DMN, CEA Saclay, F91191 Gif-sur-Yvette Cedex, France

(Received 15 November 2007; revised manuscript received 9 May 2008; published 12 August 2008)

Separating the surface segregation enthalpy into three elementary contributions (cohesive, alloy, and size) has been proposed by many authors but rarely tested quantitatively. A three element separation rule has been derived from a tight-binding Hamiltonian 15 years ago. It has yielded very satisfying results for various environments (close-packed surfaces, vicinal surfaces, grain boundaries, and clusters) for the Cu-Ag system and for many other alloys. However recently this rule has stumbled over the Co-Pt system. We therefore develop an approach—the coupled three effects model (CTEM)—based on a systematic study of the properties of permutation enthalpies—both in the bulk and in the surface—as a function of the value of the mixed interaction involved in the *N*-body interatomic potentials derived from the second moment approximation of the tight-binding scheme. We show that both the disagreement previously observed for Co-Pt and the agreement mentioned above for Cu-Ag can be explained by the variation of the alloy effective pair interactions (EPIs) in the surface and by the existence of coupling coefficients between the three effects. We also show that the surface EPIs are proportional to the bulk EPIs when the difference of atomic radii of the components can be neglected, while they differ from an additive constant in the presence of a large size effect. We suggest general criteria to determine alloys where the present improvements are expected to be significant.

DOI: 10.1103/PhysRevB.78.075413 PACS number(s): 68.35.−p, 05.70.Np, 68.35.bd, 82.60.Lf

I. INTRODUCTION

Since Gibbs'[1] famous works on the thermodynamical description of surfaces, many experimental and theoretical studies have focused on interfacial segregation (surface and grain boundary).[2–5] Segregation has indeed a strong influence on many mechanical (intergranular fracture) or chemical properties (modification of the catalytic properties with the superficial composition). Very recent papers also emphasized the role of segregation in the chemical composition of the different superficial sites of nanoclusters.[6–9]

As the nature of the segregating element in an alloy A_cB_{1-c} can depend on the bulk concentration c, statistical physics tools are required to express the surface concentration as a function of c.[4,5,10] Nevertheless, in the infinitely dilute limits, the nature of the segregating element can be determined by the segregation enthalpy ΔH_{seg}, which is defined as the energy balance of the exchange of a solute atom in the bulk with a solvent atom in the surface. *Ab initio* computations or calculations based on *N*-body interatomic potentials that are derived from the electronic structure lead to realistic values of ΔH_{seg} without allowing one to specify the physical parameters that govern the segregation.[11]

Various approaches have been proposed to interpret the segregation enthalpy. Rigid-lattice approaches with pair interactions emphasize the role of the difference of surface energies and the mixing energy.[10] A similar conclusion is obtained from a tight-binding Hamiltonian on a rigid lattice treated by the generalized perturbation method leading to the TBIM (tight-binding Ising model).[12,13] Indeed, the two energetic parameters that occur in this approach are the surface local field equivalent to the difference of surface energies and the effective pair interactions (EPIs) that govern the mixing energy.

Wynblatt and Ku[14,15] proposed to add an elastic term to these energetic parameters, in order to account for the difference of size between the components. This generalizes the McLean[16] model developed for grain boundaries. If this three effects model renders the nature of the segregating element reasonably well,[15] the authors did not validate it quantitatively by comparing the segregation energies determined from interatomic potentials to those obtained by this three effects rule via the same potentials.

More recently, Berthier *et al.*[17] developed a mixed approach (denoted BLT in the following) that generalizes the results of the TBIM by incorporating a size effect when the atomic radii of the components differ. Unlike Wynblatt and Ku,[18] this size effect is not evaluated within the linear elasticity framework but via numerical simulations using *N*-body interatomic potentials derived from the electronic structure so that the dissymmetry between tension and compression can in particular be accounted for. The reconstitution of ΔH_{seg} via this three effects rule has been compared with its direct computation via *N*-body interatomic potentials based on the second moment approximation of the tight-binding scheme, mostly for the Cu-Ag system. For surfaces of differ-

ent orientations,[17,19–21] grain boundaries,[17,22,23] and the different superficial sites of clusters,[9] it leads to a quantitative agreement since the maximal observed deviation does not exceed 50 meV for quantities that can reach 700 meV. A similar agreement has also been obtained for a series of transition-metal alloys with low mixing energies.[24,25] However, this rule recently revealed deviations of about 200 meV for quantities that are only a few tenths of millielectron volt, while studying the (100) and (111) surfaces of the Co-Pt system. Recall that this system is characterized by a lattice mismatch that is similar to the Cu-Ag system but also by a strong tendency to order (with a critical order-disorder temperature around 1100 K for the $L1_0$ phase[26]).

This paper aims at improving the separation rule by revealing the origin of this disagreement and by clarifying the couplings between the different effects. Moreover, we extend this rule to permutation enthalpies, ΔH^p_{perm}, defined as the energetic balance related to the switch of chemical nature from a solvent atom into a solute atom on a site p. The segregation enthalpy then reduces to the difference of permutation enthalpies between the surface and the bulk: $\Delta H_{\text{seg}}=\Delta H^{\text{surf}}_{\text{perm}}-\Delta H^{\text{bulk}}_{\text{perm}}$. Testing the decomposition on the permutation enthalpies then turns out to be more drastic than testing it on the segregation enthalpies since a systematic deviation on the permutation enthalpies can be discarded by the subtraction in the segregation enthalpy.

The paper is organized as follows: In Sec. II, we first present the different models to be used and recall how to compute, via the mixed approach, the above-mentioned three effects (surface energies or cohesion, alloy, and size effects) from the interatomic potentials used for the direct computation of segregation and permutation enthalpies. Then we show how to introduce the coupling between these effects by varying the mixed interaction A-B while keeping constant the potentials of the pure metals A and B. In Sec. III, we detail the couplings between the alloy effect and each of the other two effects (cohesion and size effects), both in the bulk and in the surface. This allows us to introduce an efficient way to compute the cohesion and size effects. The resulting decomposition, called the coupled three effects model (CTEM) and denoted as D_{CTEM} in the following, is then validated in Sec. IV on the Co-Pt and Cu-Ag systems. From this satisfactory agreement we clarify the validity domain of the previous BLT separation rule, denoted as D_{BLT} in the following. This allows us to explain the disagreement observed for the Co-Pt system and the success encountered for all the cases that were previously studied with the D_{BLT} approach. Finally, in Sec. V, we draw the prospects offered by this framework toward a better understanding of the segregation driving forces for systems with both strong size and alloy effects.

II. MODELS

A. *N*-body interatomic potentials

We use N-body interatomic potentials derived from the second moment approximation (SMA) of the tight-binding scheme[27,28] to compute the permutation enthalpies. In this approach, the energy on a site n is the sum of an attractive band term that takes into account the width of the local density of electronic states,[27]

$$E_n^{\text{binding}} = -\sqrt{\sum_{m\neq n} \xi_{ij}^2 \exp\left[-2q_{ij}\left(\frac{r_{nm}}{r_{ij}^0}-1\right)\right]}, \qquad (1)$$

and a repulsive term of the Born-Mayer type,[27]

$$E_n^{\text{rep}} = \sum_{m\neq n} A_{ij} \exp\left[-p_{ij}\left(\frac{r_{nm}}{r_{ij}^0}-1\right)\right]. \qquad (2)$$

The indexes i and j specify the chemical nature of the atoms on sites n and m, r_{ii}^0 (respectively r_{jj}^0) corresponds to the equilibrium distance between first neighbors in the pure metal i (respectively j), $r_{ij}^0=\frac{r_{ii}^0+r_{jj}^0}{2}$, and r_{nm} is the distance between the sites n and m. ξ_{ij} is the effective jump integral between atoms i and j.

To study a specific system, the parameters (ξ_{ij}, q_{ij}, A_{ij}, and p_{ij}) are obtained by fitting on several bulk physical quantities (lattice parameters, cohesive energies, elastic constants, and dissolution energies for the alloy parameters);[23] otherwise, canonical parameters can be used.[27] Note that fitting the SMA parameters to experimental cohesive energies leads to an underestimation of the surface energies since it is well known that such potentials are not satisfactorily transferable from isolated atoms to bulk via surface.[29] Nevertheless, these deviations do not prevent us to describe correctly the relaxations and/or reconstruction of the low index surfaces.[30] We ensure the continuity in the computation of energies and forces by shrinking to zero the attractive and repulsive interactions via a fifth-order polynomial between the distances r_{ij}^c and $r_{ij}^{c'}$, the metals considered in the present study being all in the fcc structure. For $i=j$, these distances stand, respectively, for the distances between second and fourth neighbors of the pure metal i. For $i\neq j$, we ascribe r_{ij}^c to the distance between second neighbors of the element with the largest atomic radius and $r_{ij}^{c'}$ to the distance between the fourth neighbors of the element with the smallest atomic radius. The resulting parameter values for the Cu-Ag and the Co-Pt systems are gathered in Table I. To relax the atomic posi-

TABLE I. Parameters of the interatomic potentials used for the Cu-Ag and Co-Pt systems. The quantities used for the fit [atomic radii r_{ij}^0 (Ref. 32), cohesion energies E_{coh} (Ref. 32), and bulk moduli K (Ref. 33)] are also indicated.

	A_{ij} (eV)	p_{ij}	ξ_{ij} (eV)	q_{ij}	r_{ij}^0 (Å)	E_{coh} (eV)[a]	K (GPa)
Ag-Ag	0.125	10.35	1.267	3.42	2.89	−2.95	108
Cu-Cu	0.108	10.38	1.343	2.63	2.56	−3.50	142
Ag-Cu	0.119	10.36	1.300	3.03	2.725		
Co-Co	0.189	8.80	1.907	2.96	2.50	−4.45	204
Pt-Pt	0.242	11.14	2.506	3.68	2.76	−5.86	296
Co-Pt	0.245	9.97	2.386	3.32	2.63		

[a]Note however the limitation of fitting interatomic potentials on E_{coh} as expressed in Ref. 29.

tions, we use a quenched molecular-dynamics algorithm that minimizes the potential energy at 0 K.[31]

B. Three effects rule (BLT model)

First let us consider a very simple model of nearest-neighbors pair interactions on a rigid lattice. The permutation enthalpy of an atom of the matrix B into a solute atom A for a site p (p=bulk or surface) in the limit of the infinitely dilute alloy $B(A)$ then writes: $\Delta H^p_{\text{perm}}=Z^p(V_{AB}-V_{BB})$, where Z^p is the coordination number of the site p. This expression can be rewritten as

$$\Delta H^p_{\text{perm}} = \Delta H^p_{\text{perm,coh}} + \Delta H^p_{\text{perm,alloy}}, \tag{3}$$

which brings out one term to be related to the difference of interaction energies in the pure metals A and B: $\Delta H^p_{\text{perm,coh}}=Z^p\tau=Z^p(V_{AA}-V_{BB})/2$ (cohesive effect) and a second one to be linked to the EPI: $\Delta H^p_{\text{perm,alloy}}=-Z^pV$, with $V=(V_{AA}+V_{BB}-2V_{AB})/2$ (alloy effect). However, this introduces a two-solute term V_{AA} in an artificial way since ΔH^p_{perm} only involves one solute atom in the infinitely dilute limit.

Such a pairwise description of the cohesive energy of transition metals is quite unrealistic; it was then proposed to derive a better grounded model from the electronic structure (tight-binding scheme) suited to account for the energetics of A-B permutations, still on a rigid lattice. This led to the effective Ising-like TBIM model,[12,13] which introduces the following changes with respect to Eq. (3): (i) The expression of the cohesion effect $\Delta H^p_{\text{perm,coh}}$ is generalized to the case of nonadditive interactions derived from N-body potentials. Thus the term $Z^p\tau$ issued from pair interactions between nearest neighbors on a rigid lattice is replaced by

$$\Delta H^p_{\text{perm,coh}} = H^p_A - H^p_B, \tag{4}$$

where H^p_i is the energy of the site p in the pure metal i.[4,17,23] (ii) The alloy term $\Delta H^p_{\text{perm,alloy}}=-Z^pV$ is generalized by taking into account the EPIs between kth neighbors V_k (Ref. 34) so that one writes

$$\Delta H^p_{\text{perm,alloy}} = -\sum_k Z^p_k V^p_k, \tag{5}$$

where Z^p_k is the coordination number for the kth neighbors. The EPIs V^p_k are evaluated via the N-body interatomic potential by computing the enthalpy difference ΔH_k between an initial configuration where two solute atoms are not interacting and a final configuration where the solute atoms are in the position of kth neighbors: $V^p_k=\Delta H_k/2$.[4,17,23] The enthalpies of the initial and final configurations are obtained after optimizing the atomic positions. This is the core of this dual approach that introduces the role of atomic relaxations in a rigid-lattice framework. Moreover, one can easily integrate in Eq. (5) the variation of the EPIs at the surface that is predicted both by computations based on a detailed description of the electronic structure[11,35] and by those using the N-body potentials as described above.[4,36]

Equation (3) being obtained in a rigid-lattice framework, Wynblatt and Ku[14,15] proposed to add a contribution due to the difference of size between the components, $\Delta H^p_{\text{perm,size}}$, by estimating it in the bulk via the linear elasticity formalism[37] and by assuming that it vanishes in the surface. This contribution was later improved by computing it via numerical simulation by selecting a set of parameters for the N-body potentials that are identical for the matrix (B) and the solute (B^*), except for the atomic radii of the two components for which the equilibrium values, r^0_{BB} and $r^0_{B^*B^*}=r^0_{AA}$, are considered.[18,38] The corresponding size contribution is then written as

$$\Delta H^p_{\text{perm,size}} = H^p_{\text{tot}}[B(B*)] - H_{\text{tot}}(B), \tag{6}$$

where $H^p_{\text{tot}}[B(B*)]$ is the total energy of the system with a B^* impurity at site p and $H_{\text{tot}}(B)$ is the total energy of the pure B system.

The permutation enthalpy at the site p can then be written as the sum of three terms:

$$\Delta H^p_{\text{perm}} = \Delta H^p_{\text{perm,coh}} + \Delta H^p_{\text{perm,alloy}} + \Delta H^p_{\text{perm,size}}, \tag{7}$$

in which the three contributions are given, respectively, by Eqs. (4)–(6).

This decomposition turned out to be remarkably pertinent for the different environments of the Cu-Ag system (close-packed surfaces,[17,19,20] vicinal surfaces,[21] grain boundaries,[17,22,23] and clusters of different structures[9]). Since this procedure is inductive, a deeper analysis is required to control the validity domain of the decomposition. Among the main points to be analyzed let us cite the possible coupling between size and alloy effects. Indeed, for the decomposition to be valid, the alloy effect—due to possible nonzero EPIs for the system matrix virtual solute, i.e., B-B^*—should not occur while introducing a virtual solute atom for the computation of the size effect. If this induced alloy effect turns out to be negligible for Cu-Ag,[9,22,23] this may not be the case for other systems. Strong deviations between the direct computation ΔH^p_{perm} and the proposed decomposition given by Eq. (7) can also come from Eq. (3), where a solute-solute interaction V_{AA} is introduced both in the cohesion effect $[Z^p\tau=Z^p(V_{AA}-V_{BB})/2]$ and in the alloy effect $[-Z^pV=-Z^p(V_{AA}+V_{BB}-2V_{AB})/2]$, although it does not occur in the permutation enthalpy of an isolated A solute atom $[Z^p(V_{AB}-V_{BB})]$. This results in a possible source of discrepancy between the one-solute computation employed while evaluating directly ΔH^p_{perm}, the two-solute computations to evaluate V in Eq. (5) or the evaluation of the cohesion energy in the pure metal A in Eq. (4). This is also true for atomic relaxations in the presence of a size effect since the interaction of displacement fields of two solute atoms that occurs in the computation of V does not play any role in the direct computation with only one solute atom.

C. How to couple the three effects

The problems encountered using the BLT decomposition of the permutation energy given by Eq. (7) are essentially attributed to the oversimplified assumption of decoupling the alloy contribution [Eq. (5)] from the cohesion [Eq. (4)] and size [Eq. (6)] ones. To solve them, we then need to go beyond this assumption by adopting a procedure that allows us to properly account for the coupling between these three ef-

fects, which comes from the N-body character of the interatomic potential on one hand and atomic relaxations on the other hand.

To this aim, we need to define a parameter that accounts for the alloying tendency of the system under study and that can be varied on a sufficiently large range to allow us to explore systems that tend to order or phase separate while relying on the same potentials of pure metals A and B. This is achieved here by choosing $\xi^*_{AB}=\xi_{AB}/\sqrt{\xi_{AA}\xi_{BB}}$, with ξ_{AB} being the parameter of the mixed interaction in Eq. (1). Indeed, varying ξ^*_{AB} for a given couple of A and B pure metals—defined by their cohesion and size mismatch characteristics, i.e., by the numerical values of $\Delta\xi/\xi=(\xi_{AA}-\xi_{BB})/\xi_{BB}$ (cohesion effect) and $\Delta r/r=(r^0_{AA}-r^0_{BB})/r^0_{BB}$ (size effect)—will allow the AB system to present a tendency either to order ($\xi^*_{AB}\gg 1$) or to phase separate ($\xi^*_{AB}\ll 1$).

The procedure that we adopt is then the following: We still decompose the permutation energy into three contributions, following Eq. (7):

$$\Delta H^p_{\mathrm{perm}}(\xi^*_{AB})=\Delta H^p_{\mathrm{perm,coh}}+\Delta H^p_{\mathrm{perm,alloy}}(\xi^*_{AB})+\Delta H^p_{\mathrm{perm,size}}, \tag{8}$$

in which only the alloying term depends on ξ^*_{AB}. This alloying term is modified in two manners with respect to the previous one [Eq. (5)]: (i) we separate the short-range EPIs $V^p_k(\xi^*_{AB})$ and ($k\leq k_0$)—which strongly vary with ξ^*_{AB} and therefore indeed account for the alloying effect—from the long range ones, ($k>k_0$), which do not vary with ξ^*_{AB} [$V^p_k(\xi^*_{AB})\approx V^p_k$] and therefore only depend on cohesion and size effects.[39] For the alloying term, we restrict the summation $\Sigma_k Z^p_k V^p_k$ to the short-range ξ^*_{AB}-dependent EPIs ($k\leq k_0$). (ii) To take into account a possible coupling between the three effects, we group all the dependencies of $\Delta H^p_{\mathrm{perm}}(\xi^*_{AB})$ on the alloying parameter ξ^*_{AB} into the alloying term. This introduces a coupling coefficient $\alpha^p(\xi^*_{AB})$ defined in the following manner:

$$\Delta H^p_{\mathrm{perm,alloy}}(\xi^*_{AB})=-[1+\alpha^p(\xi^*_{AB})]\sum_{k\leq k_0} Z^p_k V^p_k(\xi^*_{AB}). \tag{9}$$

In absence of coupling between the three effects, $\alpha^p(\xi^*_{AB})=0$ and Eq. (5) is recovered. We will see in the following that a major result of this approach is that $\alpha^p(\xi^*_{AB})$ does not depend on ξ^*_{AB}. It means that the coupling coefficient is a property that only depends on the characteristics of the pure metals.

Note that such a description allows us to provide a rigorous definition of the pure cohesion/size contributions from the value of the permutation enthalpy that corresponds to a nil alloy effect. More precisely,

$$\Delta H^p_{\mathrm{perm,coh}}+\Delta H^p_{\mathrm{perm,size}}=\Delta H^p_{\mathrm{perm}}(\xi^{*,p}_{AB,0}), \tag{10}$$

where $\xi^{*,p}_{AB,0}$ is defined by

$$\sum_{k\leq k_0} Z^p_k V^p_k(\xi^{*,p}_{AB,0})=0. \tag{11}$$

The key point of such a procedure is then to determine both the cut-off k_0 for alloying EPIs and their coupling coefficient with cohesion and size effects $\alpha^p(\xi^*_{AB})$, and for a system AB defined by its cohesion characteristics $\Delta\xi/\xi$ and its size mismatch $\Delta r/r$. To this aim, both the EPIs $V^p_k(\xi^*_{AB})$ and the permutation enthalpies $\Delta H^p_{\mathrm{perm}}(\xi^*_{AB})$ will be computed as a function of ξ^*_{AB} via the methods described in the previous section.

To separate univocally the couplings between the different effects (i.e., cohesion, size, and alloying) from the influence of broken bonds in the surface, we will first apply our procedure on the bulk ($p=b$). Moreover, in order to identify the respective role of the coupling between cohesion and alloy effects on one hand and size and alloy effects on the other hand, we will first detail separately these couplings by performing the calculations for virtual AB systems, whose A and B components differ either by their cohesive energy or by their size mismatch. The procedure will then be applied for the (100) surface ($p=s$). This will allow us to determine the coupling coefficients $\alpha^p_{\mathrm{coh/alloy}}$ and $\alpha^p_{\mathrm{size/alloy}}$ in both (bulk, surface) cases in order to revisit the three effects rule for surface segregation. Finally, the procedure will be generalized to couplings between the three effects and applied to the Co-Pt and Cu-Ag systems. The keypoint of all this study is the systematic variation of ξ_{AB} that allows one to define the pertinent coupling coefficients and their variations as a function of the difference in cohesive energies and the lattice mismatch.

III. DIFFERENT COUPLINGS

In this section, we will first study separately the coupling between alloying and cohesion effects on the one hand and between alloying and size effects on the other hand, before generalizing to the peculiar cases of Co-Pt and Cu-Ag, for which the three effects simultaneously occur. In all cases, the calculations will be performed in an fcc bulk then at the (100) surface. To define systems in which only cohesion or size effect occurs, we proceed as follows: (i) *No size effect*: the two metals A and B are represented by interatomic potentials leading to the same equilibrium parameter. In practice, we fix $r^0_{AA}=r^0_{BB}$ and we use the canonical values: $p_{AA}=p_{AB}=p_{BB}=9$ and $q_{AA}=q_{AB}=q_{BB}=3$.[27] Moreover, we consider values of $\Delta\xi/\xi=(\xi_{AA}-\xi_{BB})/\xi_{BB}$ that lay between −33% and +33% in order to explore the characteristic range of cohesion energies of transition metals. More precisely we chose $\xi_{BB}=1.8$ eV for the solvent—corresponding to a cohesion energy that equals −4.2 eV—while for the solute ξ_{AA} can vary between $\xi_{AA}=1.2$ eV (cohesion energy equals −2.8 eV) and $\xi_{AA}=2.4$ eV (cohesion energy of −5.6 eV). The parameters A_{ii} are obtained via the equilibrium equation[28] and $A_{AB}=\sqrt{A_{AA}A_{BB}}$.[25] (ii) *No cohesion effect*: the two metals A and B are represented by the same interatomic potentials, apart from the atomic radii. We ascribe for the solute A: $\Delta r/r=(r^0_{AA}-r^0_{BB})/r^0_{BB}=\pm 5\%$, $\pm 10\%$, and $\pm 15\%$. The parameters that are common to both pure metals A and B correspond to the copper characteristics (Table I)—from which this study has been initiated—whereas A_{AB} is taken equal to $\sqrt{A_{AA}A_{BB}}$.[25]

Then, we compute the EPIs and the permutation enthalpies as a function of ξ^*_{AB} for the above set of values of either $\Delta\xi/\xi$ in the former case and of $\Delta r/r$ in the latter case.

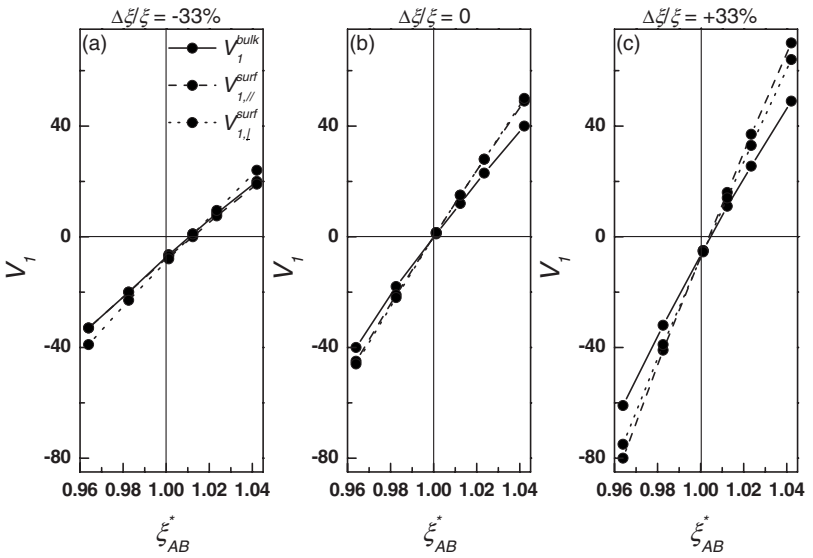

FIG. 1. Comparison of $V_{1,\parallel}^{\mathrm{surf}}$ (dashed lines), $V_{1,\perp}^{\mathrm{surf}}$ (dotted lines), and V_1^{bulk} (continuous lines), in millielectron volt, as a function of ξ_{AB}^* for pure cohesion effect (a) $\Delta\xi/\xi=-33\%$, (b) 0%, and (c) +33%.

A. EPIs

We compute first the EPIs via the method described in the previous section; we bring closer (in k-neighbor positions) two solute atoms that were initially not interacting, and we compute the energy balance after relaxing the atomic positions. Three types of EPIs are determined depending on that the two impurities both occupying either the bulk or surface sites, the first one a surface site and the other one a subsurface site, leading, respectively, to V_k^{bulk}, $V_{k,\parallel}^{\mathrm{surf}}$, and $V_{k,\perp}^{\mathrm{surf}}$. Let us discuss our main results in the case of the nearest-neighbor interaction ($k=1$), which is by far the predominant one for the fcc structure. The variations of V_1 as a function of ξ_{AB}^* are displayed in absence of size effects (Fig. 1) and in absence of cohesion effect (Fig. 2). Three situations are exhibited in each case: (i) no size effect: $\Delta\xi/\xi=-33\%$ (solute less cohesive than the matrix), 0%, and +33% (solute more cohesive than the matrix). (ii) no cohesion effect: $\Delta r/r=-10\%$ (solute smaller than the matrix), 0%, and +10% (solute bigger than the matrix).

We first analyze the bulk case. In both situations, the variations of V_1 with ξ_{AB}^* are nearly linear despite the N-body character of the interatomic potentials and despite the relaxations that strongly decrease the value of V_1 for the size effect case (they diminish the tendency to order or increase the tendency to phase separate[36]).

In the absence of size effect, for a given value of ξ_{AB}^*, $|V_1|$ tends to increase when the solute is more cohesive than the matrix and to decrease in the reverse case (apart from the shift of the zero value of V_1 that deviates slightly from the value $\xi_{AB}^*=1$ for $\Delta\xi/\xi\neq 0$) (Fig. 1). In that case, the influence of the relaxations is rather negligible and the interactions beyond V_2 are almost equal to zero although V_2 is already very small compared to V_1 ($V_2/V_1\approx 0.1$).

In the absence of cohesion effect, for a given value of $\Delta r/r$, the difference in the atomic radii increases $|V_1|$ when the solute is larger than the matrix and decreases in the reverse case (apart from the zero value of V_1 that slightly deviates from $\xi_{AB}^*=1$ for $\Delta r/r\neq 0$, as in the case $\Delta\xi/\xi\neq 0$) (Fig. 2).

We find that only V_1 and V_2 (which remains always smaller than V_1, except near the zero value of V_1) depend significantly on ξ_{AB}^*. This indicates that the sum of the EPIs that occurs in Eq. (9) to determine $\Delta H_{\mathrm{perm,alloy}}^{\mathrm{bulk}}$ can be re-

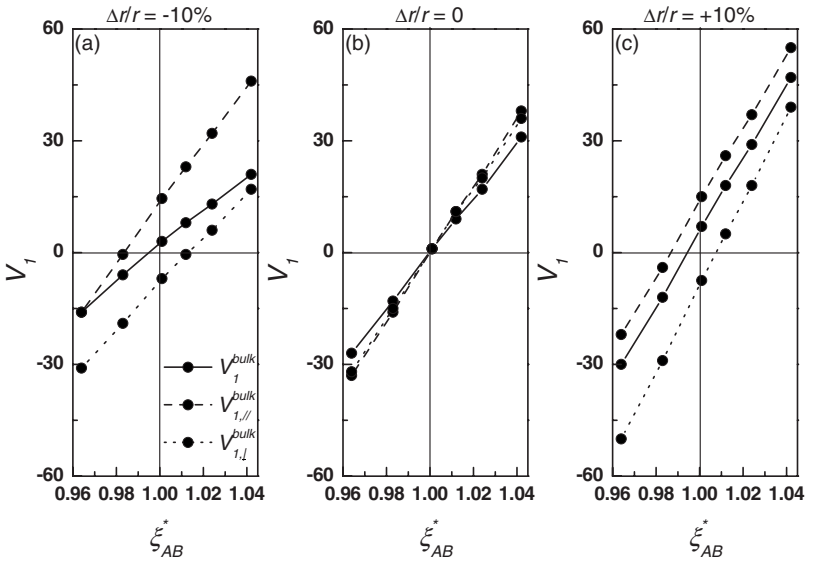

FIG. 2. Comparison of $V_{1,\parallel}^{\mathrm{surf}}$ (dashed lines), $V_{1,\perp}^{\mathrm{surf}}$ (dotted lines), and V_1^{bulk} (continuous lines), in millielectron volt, as a function of ξ_{AB}^* for pure size effect (a) $\Delta r/r=-10\%$, (b) 0%, and (c) +10%.

stricted to $k \leq k_0 = 2$. For $k \geq 3$, the very weak remaining EPIs do not depend on the alloy mixed interactions but only on $\Delta\xi/\xi$ or $\Delta r/r$.

We now comment on our results in the surface case. Tight-binding computations with a detailed description of the electronic density of states but without atomic relaxations emphasized that the alloy EPIs were strengthened in the surface. This holds true both for the interactions in the surface plane and for those between sites in the surface plane and sites in the underlying plane.[12,13] This tight-binding result has been confirmed later by *ab initio* computations.[11,35]

In absence of both cohesion and size effects ($\Delta\xi/\xi = \Delta r/r = 0$), Figs. 1 and 2 show that $V_{1,\parallel}^{\text{surf}} \approx V_{1,\perp}^{\text{surf}} \approx 1.2 V_1^{\text{bulk}}$, in good agreement with the computations mentioned above. When only the cohesive energies differ ($\Delta r/r = 0$), the multiplicative factor between $V_{1,\parallel}^{\text{surf}} \approx V_{1,\perp}^{\text{surf}}$ and V_1^{bulk} is maintained, but it slightly increases for $\Delta\xi/\xi > 0$ [Fig. 1(c)] and diminishes in the reverse case [Fig. 1(a)]. However, a difference in the atomic radii of the components radically modifies this behavior. Indeed, for $\Delta r/r = +10\%$, the multiplicative factor between V_1^{surf} and V_1^{bulk} is replaced by additive factors. More precisely, $V_{1,\parallel}^{\text{surf}} - V_1^{\text{bulk}} \approx 8$ meV and $V_{1,\perp}^{\text{surf}} - V_1^{\text{bulk}} \approx -14$ meV [Fig. 2(c)]. For $\Delta r/r = -10\%$, Fig. 2(a) displays an intermediate behavior resulting simultaneously from a multiplicative and an additive factor (positive for $V_{1,\parallel}^{\text{surf}}$ and negative for $V_{1,\perp}^{\text{surf}}$), the latter prevailing when $|\Delta r/r|$ increases.

B. Cohesion and size contributions

The permutation enthalpies have also been calculated in both cases (no size effect and no cohesion effect), for the same values of $\Delta\xi/\xi$ and $\Delta r/r$. The main result is that they vary linearly with ξ_{AB}^*. From the EPIs calculated in the previous section, we derive the variation with ξ_{AB}^* of the sum of EPIs involved in the contribution of the alloy effect $-\Sigma_{k\leq 2} Z_k^p V_k^p$ [cf. Eq. (9)]. From this variation that is also linear, we can determine the value $\xi_{AB,0}^{*,p}$ for which this sum vanishes, corresponding to a nil alloy effect. The value of $\Delta H_{\text{perm}}^p(\xi_{AB,0}^{*,p})$ then gives us, respectively, (i) no size effect: the cohesion effect $\Delta H_{\text{perm,coh}}^p$, which is found here to be almost equal to that obtained via the classical approach, i.e., to $H_A^p - H_B^p$, where H_i^p is the site energy in the pure metal i, see Eq. (4). Recall that the equality holds for pair interactions on a rigid lattice. Since this results holds for both bulk and surface sites, $\Delta H_{\text{seg,coh}} (= \Delta H_{\text{perm,coh}}^{\text{surf}} - \Delta H_{\text{perm,coh}}^{\text{bulk}})$ equals the expression previously proposed for the contribution of the cohesion effect to the segregation enthalpy,[4,17,22,23] which reduces to the double difference between the energies of the surface and bulk sites for the pure metals A and B. This term is equal to the difference of the surface energies of the metals A and B if the bulk energy is recovered for the first underlying plane under the surface, which is rather true for close-packed surfaces of transition metals; and (ii) no cohesion effect: the size effect $\Delta H_{\text{perm,size}}^p$, which is plotted for p = bulk site as a function of $\Delta r/r$ in Fig. 3(a), before and after relaxations. $\Delta H_{\text{perm,size}}^{\text{bulk}}$ is also compared with the value deduced from the continuous linear elasticity:[37]

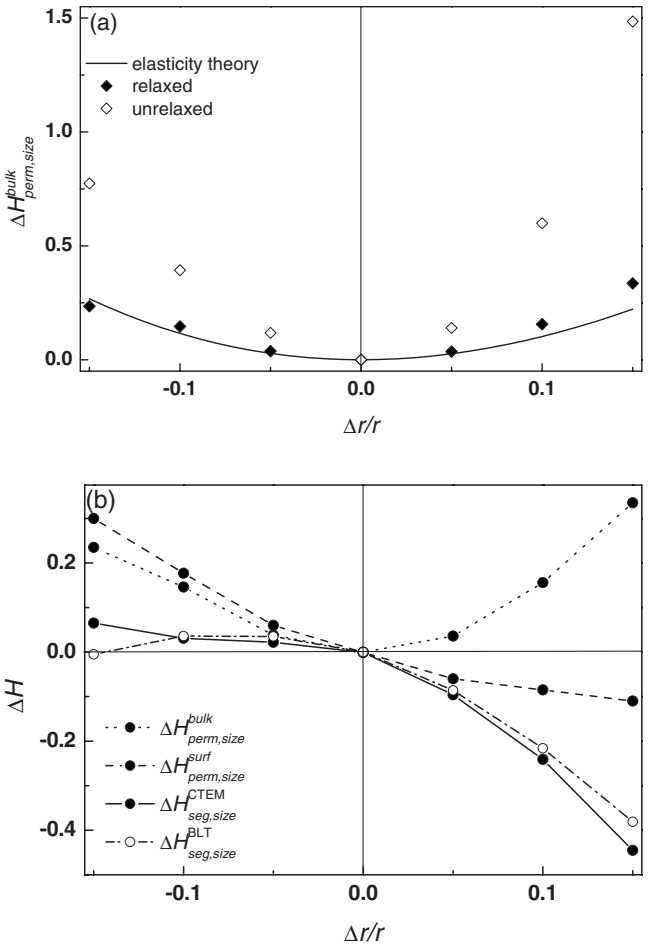

FIG. 3. Size effect contribution (in eV/at): (a) $\Delta H_{\text{perm,size}}^{\text{bulk}}$ without (empty symbols) and with (full symbols) relaxations of atomic positions as a function of $\Delta r/r$. Our atomistic calculations are compared with the values given by elasticity theory (continuous lines). (b) $\Delta H_{\text{perm,size}}^{\text{surf}}$ (dashed lines), $\Delta H_{\text{perm,size}}^{\text{bulk}}$ (dotted lines), $\Delta H_{\text{seg,size}}^{\text{CTEM}}$ (continuous lines with full symbols), and $\Delta H_{\text{seg,size}}^{\text{BLT}}$ (continuous lines with empty symbols) as a function of $\Delta r/r$. Energies are expressed in electron volt.

$$\Delta H_{el} = \frac{24\pi K_A G_B r_A^0 r_B^0 (r_B^0 - r_A^0)^2}{3K_A r_A^0 + 4G_B r_B^0}, \tag{12}$$

where K_A and G_B are, respectively, the bulk modulus of the solute (with atomic radius r_A^0) and the shear modulus of the matrix (with atomic radius r_B^0). For $|\Delta r/r| < 5\%$, the elastic theory provides a very satisfactory approximation of $\Delta H_{\text{perm,size}}^{\text{bulk}}$. Beyond 10%, the dissymmetry tension-compression due to the anharmonicity of the potential leads to larger values for a solute atom that is larger than the matrix ($\Delta r/r > 0$) than in the reverse case for the same value of $|\Delta r/r|$, which could not be obtained via the elastic computations. Moreover, one can note the crucial role of the relaxations in the estimation of $\Delta H_{\text{perm,size}}^{\text{bulk}}$; in particular, the larger $|\Delta r/r|$ is, the more the relaxations diminish the value of $\Delta H_{\text{perm,size}}^{\text{bulk}}$. Figure 3(b) gathers the contributions of the size effect to the permutation enthalpies in the surface and in the bulk, and to the segregation enthalpy. As shown by the con-

traction of the interplanar distance between the surface plane and the first underlayer,[28,40] the surface plane is in tension for the stress components parallel to the surface. This results in a gain in the permutation enthalpy $\Delta H^{surf}_{perm,size}<0$ when the solute is bigger than the matrix and a loss in the reverse case. We also show the values of $\Delta H_{seg,size}$ obtained via the BLT method on Fig. 3(b),[17,22,23] which exhibit significant deviations from the CTEM ones for large differences in atomic radii ($|\Delta r/r|>10\%$) only. In this case, the BLT method slightly underestimates $|\Delta H_{seg,size}|$. We can now explain the strong dissymmetry of the component $\Delta H_{seg,size}$ of the segregation enthalpy from this analysis. Thus, for $\Delta r/r>0$, the energy gain in surface and the energy loss in the bulk lead to a large gain for the segregation enthalpy ($\Delta H_{seg,size}<0$) [Fig. 3(b)]. Reversely, for $\Delta r/r<0$, the energy loss is rather equivalent in the surface and in the bulk, which leads to values of $\Delta H_{seg,size}$ that are slightly positive. Two comments on frequent ideas encountered in the literature arise from these results. First, the dissymmetry of the segregation enthalpy as a function of $\Delta r/r$ is not essentially due to the anharmonicity of the interatomic potential and its dissymmetry between tension and compression. As shown before, this effect only explains the slight asymmetry of $\Delta H^{bulk}_{perm,size}$, while the dissymmetry of $\Delta H_{seg,size}$ comes mainly from the sign reversal of $\Delta H^{surf}_{perm,size}$ with the sign of $\Delta r/r$, which is due to the tensile surface stress. Second, the McLean[16] assumption that has initially been proposed for intergranular segregation and extended to surface segregation by Wynblatt and Ku[14,15] is somewhat too simple. These authors suggest that the elastic energy corresponding to a solute atom in the bulk [elastic approximation of $\Delta H^{bulk}_{perm,size}$, Eq. (12)] is completely relaxed in the surface, which leads to $\Delta H_{seg,size}=-\Delta H^{bulk}_{perm,size}$. Figure 3(b) shows that this approximation that neglects the role of $\Delta H^{surf}_{perm,size}$ strongly underestimates $|\Delta H_{seg,size}|$ for $\Delta r/r>0$ and overestimates $|\Delta H_{seg,size}|$ for $\Delta r/r<0$, with even a sign error in this last case.

C. Coupling coefficient

The linear variations observed both for the permutation enthalpies and for the summation of the alloying EPIs ($-\Sigma_{k\leq 2}Z^p_k V^p_k$) as a function of ξ^*_{AB} imply that the coupling coefficient α^p does not depend on ξ^*_{AB} [see Eqs. (8) and (9)]. *This is a major result, which indicates that the coupling coefficient depends only on the potentials of the pure metals A* and *B*. This allows us to study the variation of the coupling coefficient between cohesion and alloying effects, $\alpha^p_{coh,alloy}$, as a function of $\Delta\xi/\xi$ when $\Delta r/r=0$ and the variation of $\alpha^p_{size,alloy}$ as a function of $\Delta r/r$ when $\Delta\xi/\xi=0$. Figure 4(a) shows the variation of $\alpha^{bulk}_{coh,alloy}$, both in the bulk and in the surface. For $\Delta\xi/\xi>0$ (respectively $\Delta\xi/\xi<0$) [solute more (respectively less) cohesive than the matrix], $\alpha^{bulk}_{coh,alloy}$ is negative (respectively positive) and quite proportional to $\Delta\xi/\xi$. It diminishes (respectively increases) the contribution of the alloy effect (in absolute value) in ΔH^{bulk}_{perm}. For $|\Delta\xi/\xi|=33\%$ this correction reaches 15%. As the atomic relaxations affect slightly the values of ΔH^{bulk}_{perm} when the atomic radii of the two elements are equal, one can conclude that this coefficient mainly comes from the *N*-body feature of the interatomic potentials. Indeed, for pair interactions on a rigid lattice, $\alpha^{bulk}_{coh,alloy}$ equals zero by definition.

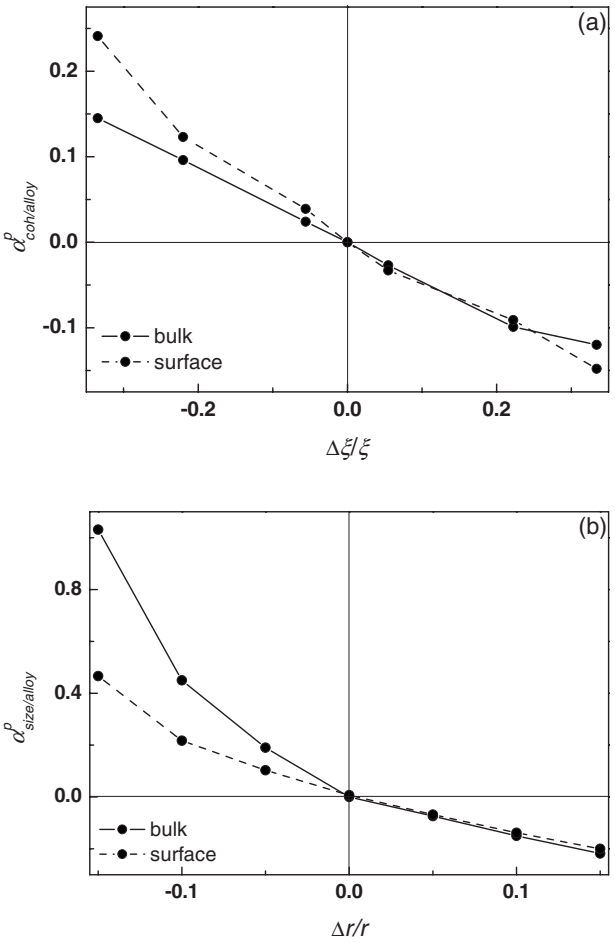

FIG. 4. Coupling coefficient for (a) pure cohesion effect: $\alpha^p_{coh/alloy}$ as a function of $\Delta\xi/\xi$ for p=surface (dashed lines) and p=bulk (continuous lines), and for (b) pure size effect: $\alpha^p_{size/alloy}$ as a function of $\Delta r/r$ for p=surface (dashed lines) and p=bulk (continuous lines).

The same Fig. 4(a) compares the variations of $\alpha^{surf}_{coh/alloy}$ as a function of $\Delta\xi/\xi$ with the ones obtained for $\alpha^{bulk}_{coh/alloy}$. For $\Delta\xi/\xi>0$ (solute more cohesive than the matrix), we observe a rather linear variation and $\alpha^{surf}_{coh/alloy}\approx\alpha^{bulk}_{coh/alloy}$. For $\Delta\xi/\xi<0$ (solute less cohesive than the matrix), a nonlinear contribution appears for large values of $|\Delta\xi/\xi|$, leading to an increase in $\alpha^{surf}_{coh/alloy}$ with regard to the bulk value $\alpha^{bulk}_{coh/alloy}$.

In the absence of cohesion effect, $\alpha^{bulk}_{size/alloy}$ represents the coupling between the size and alloy effects, which mainly induces a deviation between the one-solute (for ΔH^{bulk}_{perm}) and two-solute computations (via the EPIs), keeping in mind that the *N*-body feature of the interatomic potentials is still acting. Figure 4(b) displays the variations of $\alpha^{bulk}_{size/alloy}$ as a function of $\Delta r/r$. For $\Delta r/r\geq 0$ (solute bigger than the matrix), $\alpha^{bulk}_{size/alloy}$ is negative and proportional to $\Delta r/r$, similarly to $\alpha^{bulk}_{site/alloy}$ for $\Delta\xi/\xi\geq 0$ (solute more cohesive than the matrix). For $\Delta r/r<0$, $\alpha^{bulk}_{size/alloy}$ is positive but varies more strongly than in the previous case, mainly because of the role of the atomic relaxations. Typically, the value reached by $\alpha^{bulk}_{size/alloy}$ for $\Delta r/r=-15\%$ doubles the contribution of the alloy effect for that value of $\Delta r/r$.

Figure 4(b) also compares the variations of $\alpha^p_{\text{size/alloy}}$ in the surface and in the bulk as a function of $\Delta r/r$. For $\Delta r/r>0$, $\alpha^p_{\text{size/alloy}}$ is almost identical in the surface and in the bulk. For $\Delta r/r<0$, the value of $\alpha^p_{\text{size/alloy}}$ in the surface is around half the value in the bulk on the range of $\Delta r/r$ considered here.

IV. COUPLED THREE EFFECTS MODEL: APPLICATION TO CO-PT AND CU-AG (100)

After having studied separately the couplings between the alloy and cohesion effects on one hand, and between the alloy and size effects on the other hand, we apply this procedure to the (100) surface of two specific systems: Co-Pt and Cu-Ag, for which the three effects are coupled. Co-Pt and Cu-Ag represent systems with very different characteristics (cf. Table I). While the difference in the atomic radii is similar in both systems ($r^0_{\text{Pt}}/r^0_{\text{Co}}\approx 1.11$ and $r^0_{\text{Ag}}/r^0_{\text{Cu}}\approx 1.13$), the larger element (Pt) is also more cohesive for the Co-Pt system; whereas the larger element is the less cohesive (Ag) in the Cu-Ag system. Moreover, the Co-Pt system displays a strong tendency to order while the Cu-Ag system is characterized by a large miscibility gap.

For these systems that present simultaneously size, alloy, and cohesion effects, we carry out the CTEM procedure proposed in Sec. II C. The EPIs and the permutation enthalpies are computed in the bulk and in the surface as a function of ξ^*_{AB}, while the interatomic potentials for the interactions Co-Co and Pt-Pt on one hand and Cu-Cu and Ag-Ag on the other hand are fixed (Table I). Similar to before, the comparison of the linear variation with ξ^*_{AB} of the quantities ΔH^p_{perm} and $\Sigma_{k<2} Z^p_k V^p_k$ allows us to define the coefficient $\alpha^p_{3\ \text{effects}}$. Here again, this coefficient is valid for all the values of ξ^*_{AB} and is independent of the specific values of ξ^*_{AB} determined for the Co-Pt and Cu-Ag systems, which leads to an unambiguous definition of alloy, cohesive, and size effects. With the EPIs and the coefficient $\alpha^p_{3\ \text{effects}}$, one can generalize relation (8) to obtain the coupled three effects model (CTEM);

$$\Delta H^p_{\text{perm}} = \Delta H^p_{\text{perm,alloy}} + \Delta H^p_{\text{perm,coh}} + \Delta H^p_{\text{perm,size}}, \quad (13)$$

with

$$\Delta H^p_{\text{perm,alloy}} = -(1+\alpha^p_{3\ \text{effects}})\sum_{k\le 2} Z^p_k V^p_k. \quad (14)$$

Moreover, relations (10) and (11) can be used to give separately the cohesion and size contributions:

$$\Delta H^p_{\text{perm,coh}} = H^p_A - H^p_B, \quad (15)$$

$$\Delta H^p_{\text{perm,size}} = \Delta H^p_{\text{perm}}\left(\sum_{k\le 2} Z^p_k V^p_k = 0\right) - (H^p_A - H^p_B). \quad (16)$$

This decomposition of the permutation enthalpy can naturally be extended to segregation enthalpies.

A. Co-Pt (100)

In view of the values of $\Delta\xi/\xi$ (cohesion effect) and of $\Delta r/r$ (size effect), and of the general behavior illustrated in Sec. III, the Co(Pt) and Pt(Co) systems can be viewed as representative of hybrid cases where the relation between surface and bulk EPIs results from the combination of a multiplicative factor (cohesion effect) with an additive one (size effect).

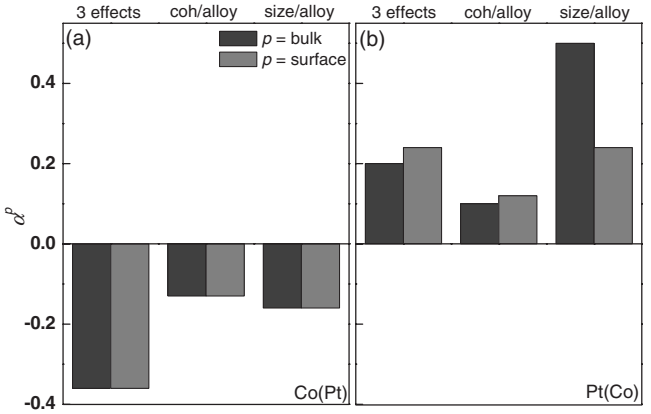

FIG. 5. $\alpha^p_{3\ \text{effects}}$ (bulk and surface) and coupling coefficients as determined in Sec. III C between cohesion and alloy effects, $\alpha^p_{\text{coh/alloy}}$, and between size and alloy effects, $\alpha^p_{\text{size/alloy}}$, for (a) Co(Pt) and (b) Pt(Co).

The values of $\alpha^p_{3\ \text{effects}}$ for the bulk and the surface computed from ΔH^p_{perm} as a function of ξ^*_{AB} are shown in Fig. 5. We also show the coupling coefficients as determined in the previous sections for the two couplings: cohesion/alloy and size/alloy. Since the bigger element (Pt) is also the more cohesive, $\alpha^p_{\text{coh/alloy}}$ and $\alpha^p_{\text{size/alloy}}$ have the same sign, which is negative for Co(Pt) and positive for Pt(Co). These signs are confirmed by the computation of $\alpha^p_{3\ \text{effects}}$ despite the nonadditivity of these coupling constants (Fig. 5).

Using formulas (13)–(16), we determine the three components of the permutation energies in the bulk and in the surface, which provide the segregation enthalpies shown in Fig. 6. The direct computation of ΔH_{seg} and its reconstitution Σ via the three components successfully agree very well, as can also be seen in Fig. 6. The deviations are smaller than 15 meV for quantities that result from competitive elementary effects that can reach 300 meV. We also give the results obtained by the previous decomposition D_{BLT}. This clearly shows that the strong disagreement observed for Co(Pt), at the origin of this study, comes rather completely from the evaluation of the contribution of the alloy effect, which is very overestimated (by more than 200 meV) by the D_{BLT} decomposition [Fig. 6(a)]. The contribution of the size effect $\Delta H_{\text{seg,size}}$ is however very comparable between both methods, as we already noticed in the previous section [cf. Fig. 2(b)].

The evaluation of the contribution of the alloy effect $\Delta H_{\text{seg,alloy}}$ differs on two points between this method and D_{BLT}: (i) considering the variation of the EPIs in the surface and (ii) considering the coupling between the three effects via $\alpha^p_{3\ \text{effects}}$.

Figure 6 stresses the importance of each of these points in the deviation observed in $\Delta H_{\text{seg,alloy}}$. For Co(Pt), the strengthening of the surface EPIs (D_{EPIp}) reduces $\Delta H_{\text{seg,alloy}}$ (of around 100 meV) and the coupling between the three effects leads to an additional reduction of 100 meV. For

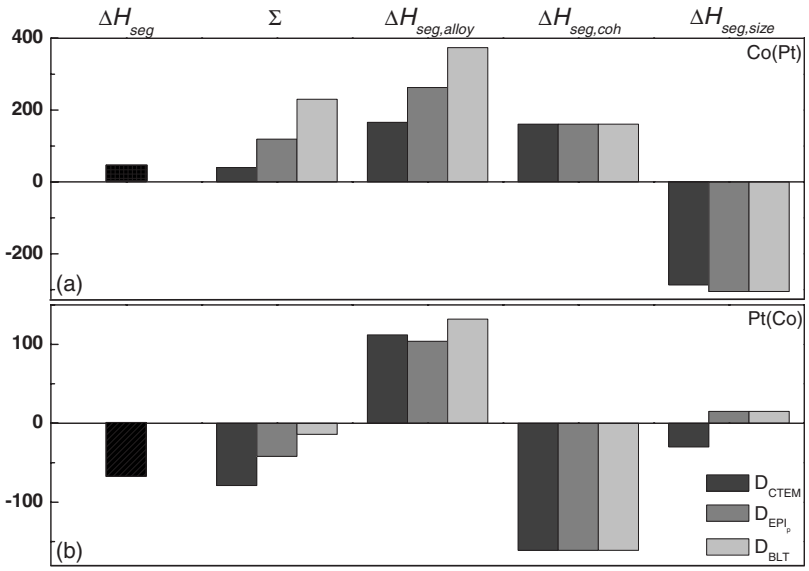

FIG. 6. Comparison between direct calculation, ΔH_{seg}, and reconstitution, Σ, of the segregation energy for (a) Co(Pt) and (b) Pt(Co) using either the D_{BLT} or the D_{CTEM} decompositions. The role of the variation of the EPIs in the surface is illustrated by the D_{EPI_p} decomposition, which gives the value of the segregation energy when only the variation of the EPIs in the surface is taken into account but not the coupling coefficients. Energies are expressed in millielectron volt.

Pt(Co), the bulk EPIs and the value of $\Delta H_{\mathrm{seg,alloy}}$ obtained by the D_{BLT} decomposition are around three times weaker than in Co(Pt). The influence of the strengthening of the surface EPIs is very close (in relative value) to the one observed for Co(Pt). However, the positive sign of $\alpha_{3\ \mathrm{effects}}^{p}$ in Pt(Co) leads to an increase in $\Delta H_{\mathrm{seg,alloy}}$ that partly compensates the previous effect. This analysis shows that determining the segregation driving forces requires specific care in systems with large values of EPIs.

B. Cu-Ag (100)

We now consider the Cu-Ag system for which the BLT decomposition was successful. Recall that this system is characterized by a strong tendency to phase separate, the larger element (Ag) being the less cohesive. Now the values of $\Delta\xi/\xi$ (cohesion effect) and of $\Delta r/r$ (size effect) make the system representative of a system with a pure size effect. Besides their positions in a $(\Delta\xi/\xi,\ \Delta r/r)$ map, it is worth noticing that the Co-Pt and Cu-Ag systems strongly differ by the value of ξ_{AB}^{*} that governs the mixed interaction A-B: for Co-Pt, $\xi_{AB}^{*}(\approx 1.09)$ is well above the value corresponding to $V_1=0$ in the bulk $(\xi_{AB}^{*}\approx 1.04)$, which is consistent with the strong tendency to the order of this system. For Cu-Ag, $\xi_{AB}^{*}(\approx 0.996)$ is very close to the value that cancels V_1 in the bulk $(\xi_{AB}^{*}\approx 1.005)$. This confirms that the wide miscibility gap observed in this system is mainly related to the size difference between Cu and Ag.

The values of $\alpha_{3\ \mathrm{effects}}^{p}$ for the bulk and the surface and the coupling coefficients for effects taken two by two are shown in Fig. 7. Due to the fact that the larger element (Ag) is also the less cohesive, $\alpha_{\mathrm{coh/alloy}}^{p}$ and $\alpha_{\mathrm{size/alloy}}^{p}$ have opposite signs. Figure 7 shows that the coupling between size and alloy effects prevails since $\alpha_{3\ \mathrm{effects}}^{p}$ is close to $\alpha_{\mathrm{size/alloy}}^{p}$.

The decomposition is proved to be valid by comparing the direct computation of ΔH_{seg} and its reconstitution Σ via the three elementary effects, as can be seen in Fig. 8. The deviations are smaller than 10 meV and the CTEM decomposition leads to results that are very similar to D_{BLT}. To understand the relative invariance of the results between both methods in this system, we detail the effects of the variations of the EPIs at the surface and of the coupling coefficient $\alpha_{3\ \mathrm{effects}}^{p}$ in $\Delta H_{\mathrm{seg,alloy}}$ such as for Co-Pt (Fig. 8).

For Cu(Ag) the variation of the EPIs parallel and perpendicular to the surface increases slightly $|\Delta H_{\mathrm{seg,alloy}}|$, while the negative value of $\alpha_{3\ \mathrm{effects}}^{p}$ has the opposite effect. This leads to a very similar estimation of $\Delta H_{\mathrm{seg,alloy}}$ between D_{BLT} and D_{CTEM}. For Ag(Cu), the variation of the EPIs at the surface diminishes $|\Delta H_{\mathrm{seg,alloy}}|$ slightly, whereas the positive value of $\alpha_{3\ \mathrm{effects}}^{p}$ has the opposite effect, leading again to a very weak modification of $\Delta H_{\mathrm{seg,alloy}}$ between D_{BLT} and D_{CTEM}.

V. DISCUSSION

The decomposition of the segregation enthalpy into three effects previously proposed (D_{BLT}) was quantitatively satisfactory for various crystallographic environments (close-packed,[17,19,20] vicinal surfaces,[21] grain boundaries,[17,22,23] and clusters[9]) in the Cu-Ag system and in

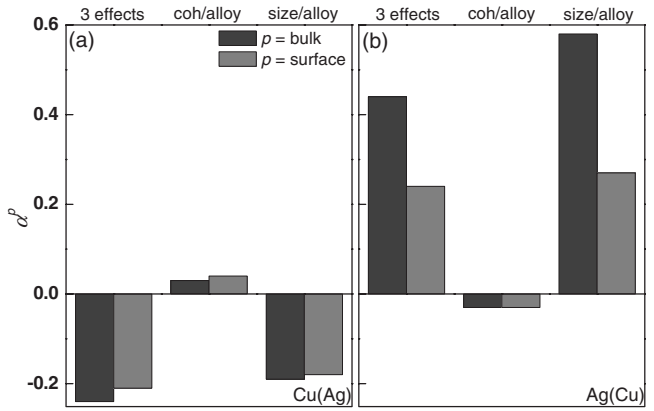

FIG. 7. $\alpha_{3\ \mathrm{effects}}^{p}$ (bulk and surface) and coupling coefficients as determined in Sec. III C between cohesion and alloy effects, $\alpha_{\mathrm{coh/alloy}}^{p}$, and between size and alloy effects, $\alpha_{\mathrm{size/alloy}}^{p}$, for (a) Cu(Ag) and (b) Ag(Cu).

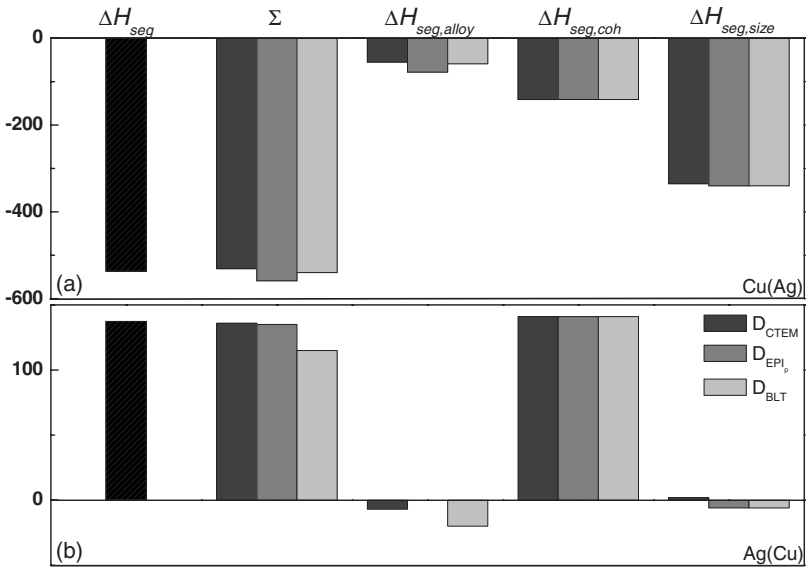

FIG. 8. Comparison between direct calculation, ΔH_{seg}, and reconstitution, Σ, of the segregation energy for (a) Cu(Ag) and (b) Ag(Cu) using either the D_{BLT} or the D_{CTEM} decompositions. The role of the variation of the EPIs in the surface is illustrated by the D_{EPI_p} decomposition, which gives the value of the segregation energy when only the variation of the EPIs in the surface is taken into account but not the coupling coefficients. Energies are expressed in millielectron volt.

many others.[24,25] Its inability to reproduce the segregation enthalpy in the case of Co(Pt) led us to develop the present approach based on a systematic study of the properties of the permutation and segregation enthalpies as a function of the value of the mixed interaction ξ_{AB} between the components A and B of the alloy, leading to the coupled three effects model.

This systematic study has revealed an unexpected property of the alloy effective pair interactions. Although it is well known that these interactions vary between the surface and the bulk,[11–13,35,36,39] no general prediction on these variations was available. This study shows that a size mismatch between the components can lead to factors that are mainly additive; the intraplane surface interactions being greater than the bulk ones, while the interplane interactions are lower. Conversely, in the absence of a size effect, our computations predict a factor that is essentially multiplicative between surface and bulk interactions, leading to a strengthening (in absolute value) of these interactions in the surface that is quite identical for the intraplane and interplane interactions. Besides, this study shows that only the interactions between nearest and next-nearest neighbors depend strongly on the mixed interaction parameter ξ_{AB}, while further interactions are governed by the size difference between the components and to a certain extent by the N-body character of the interatomic potentials. We plan to compare the values of the interactions beyond the next-nearest neighbors between direct computation and calculations based on the anisotropic elasticity.

Evaluating the contribution of the alloy effect to the permutation and segregation enthalpies in the infinitely dilute limits comes up against the following difficulty: While the computation of $\Delta H^p_{\mathrm{perm}}$ only involves one solute atom, computing $\Delta H^p_{\mathrm{perm,alloy}}$ via the EPIs relies on two-solute calculations. In particular, the interaction between the displacement fields of these two impurities plays a role in the EPI and not in $\Delta H^p_{\mathrm{perm}}$, which is very important in the presence of a size effect. We have shown that it is possible to solve this difficulty by introducing *coupling coefficients between cohesion, size, and alloy effects that only depend on the properties of the pure metals and not on the mixed interaction A-B*. We have then isolated the main characteristics of these coefficients as a function of the sign of the difference in cohesion energies and the atomic radii. The direct computation of these coefficients belongs to the prospects of this work.

The sum of the contributions of the cohesion and size effects is estimated via the permutation enthalpy for the value of ξ_{AB} that cancels the contribution of the alloy effect. After checking that the contribution of the cohesion effect $\Delta H^p_{\mathrm{perm,coh}}$ equals the difference of site energies between the pure metals A and B, we have deduced the contributions due to the size effect $\Delta H^p_{\mathrm{perm,size}}$ and $\Delta H_{\mathrm{seg,size}}$. We have shown that the dissymmetry of $\Delta H_{\mathrm{seg,size}}$ as a function of the sign of $\Delta r/r$, i.e., $|\Delta H_{\mathrm{seg,size}}|$ that is more important when $\Delta r/r>0$ (solute bigger than the matrix) than in the opposite case, comes mainly from the tensile character of the surface and not from the tension/compression dissymmetry of the interatomic potential due to its anharmonicity.

Accounting for the variation of the EPIs at the surface and the coupling coefficient between the three elementary effects (cohesion, size and alloy) leads us to propose an improved decomposition D_{CTEM} of the permutation and segregation enthalpies. This reproduces the segregation enthalpy within 20 meV, in particular in the case of the Co(Pt) system where the previous decomposition leads to a difference of about 200 meV. The improvement is essentially performed on the contribution of the alloy effect $\Delta H_{\mathrm{seg,alloy}}$. A detailed analysis explains why this is crucial for Co(Pt) and quite negligible for the Cu-Ag system. This comes from the fact that the effect of the variation of the EPIs at the surface and of the coupling go into the same direction for Co(Pt), contrary to Cu-Ag. The previous analysis of the variation of the EPIs at the surface and of the sign of $\alpha^p_{3\ \mathrm{effects}}$ indicates that the required conditions for the two effects to behave in parallel are $\alpha^p_{3\ \mathrm{effects}}<0$ and $|V^{\mathrm{surf}}|>|V^{\mathrm{bulk}}|$, which diminishes $|\Delta H_{\mathrm{seg,alloy}}|$. $\alpha^p_{3\ \mathrm{effects}}<0$ corresponds to a solute that is more cohesive [Fig. 3(a)] or bigger [Fig. 3(b)] than the matrix, while the hierarchy $|V^{\mathrm{surf}}|>|V^{\mathrm{bulk}}|$ corresponds to the most encountered situation (Figs. 1 and 2). Co(Pt) is representative of this case; $\alpha^p_{3\mathrm{effects}}>0$ and $|V^{\mathrm{surf}}|<|V^{\mathrm{bulk}}|$, which in-

creases $|\Delta H_{\mathrm{seg,alloy}}|$. $\alpha^{p}_{\mathrm{3effects}}>0$ corresponds to a solute that is less cohesive [Fig. 3(a)] or smaller [Fig. 3(b)] than the matrix in the absence of cohesion effect—while the inequality $|V^{\mathrm{surf}}|<|V^{\mathrm{bulk}}|$ can be encountered when the size effect prevails for restricted ranges of values of ξ_{AB} (Fig. 2). This last condition strongly reduces the number of systems corresponding to this case.

This analysis shows that the improvements brought to the modeling of the alloy effect by this present study shall be mainly sensitive to systems for which the values of the EPIs are large (phase diagrams with ordered compounds or coherent miscibility gap with a high critical temperature) and the solute is bigger (or more cohesive) than the matrix. For the Ni(Zr), Pt(Ti), and Pt(Zr) systems that have already been experimentally studied in the framework of superficial segregation,[41–43] this current approach is expected to be useful to establish a consistent decomposition of ΔH_{seg}. Besides, current works aim at extending this approach to grain boundaries and clusters.

ACKNOWLEDGMENTS

We thank R. Tétot for the fruitful discussions and GDR Relax for the financial support during the visit of I.B. in Marseille.

[1] J. W. Gibbs, *The Collected Works of J. W. Gibbs* (Yale University Press, New Haven, 1948), Vol. 1.
[2] Y. Gauthier and R. Baudoing, in *Surface Segregation and Related Phenomena*, edited by P. A. Dowben and A. Miller (CRC, Boca Raton, FL, 1990), p. 169.
[3] U. Bardi, Rep. Prog. Phys. **57**, 939 (1994).
[4] G. Tréglia, B. Legrand, F. Ducastelle, A. Saúl, C. Gallis, I. Meunier, C. Mottet, and A. Senhaji, Comput. Mater. Sci. **15**, 196 (1999).
[5] P. Wynblatt and D. Chatain, Metall. Mater. Trans. A **37**, 2595 (2006).
[6] M. Polak and L. Rubinovich, Phys. Rev. B **71**, 125426 (2005).
[7] G. Barcaro, A. Fortunelli, G. Rossi, F. Nita, and R. Ferrando, J. Phys. Chem. B **110**, 23197 (2006).
[8] F. Lequien, J. Creuze, F. Berthier, and B. Legrand, J. Chem. Phys. **125**, 094707 (2006).
[9] V. Moreno, J. Creuze, F. Berthier, C. Mottet, G. Tréglia, and B. Legrand, Surf. Sci. **600**, 5011 (2006).
[10] F. L. Williams and D. Nason, Surf. Sci. **45**, 377 (1974).
[11] V. Drchal, A. Pasturel, R. Monnier, J. Kudrnovsky, and P. Weinberger, Comput. Mater. Sci. **15**, 144 (1999).
[12] G. Tréglia, B. Legrand, and F. Ducastelle, Europhys. Lett. **7**, 575 (1988).
[13] F. Ducastelle, B. Legrand, and G. Tréglia, Prog. Theor. Phys. Suppl. **101**, 159 (1990).
[14] P. Wynblatt and R. C. Ku, Surf. Sci. **65**, 511 (1977).
[15] P. Wynblatt and R. C. Ku, in *Interfacial Segregation*, edited by W. C. Johnson and J. M. Blakely (ASM, Metals Park, OH, 1979), p. 115.
[16] D. McLean, *Grain Boundaries in Metals* (Oxford University Press, London, 1957), p. 116.
[17] F. Berthier, B. Legrand, and G. Tréglia, Acta Mater. **47**, 2705 (1999).
[18] D. Tomanek, A. A. Aligia, and C. A. Balseiro, Phys. Rev. B **32**, 5051 (1985).
[19] J. Creuze, F. Berthier, R. Tétot, and B. Legrand, Surf. Sci. **491**, 1 (2001).
[20] J. Creuze, F. Berthier, R. Tétot, and B. Legrand, Surf. Sci. Lett. **491**, L651 (2001).
[21] J. Creuze, F. Berthier, R. Tétot, and B. Legrand, Surf. Sci. **553**, 168 (2004).
[22] J. Creuze, F. Berthier, R. Tétot, and B. Legrand, Phys. Rev. B **62**, 2813 (2000).
[23] J. Creuze, Defect Diffus. Forum **203-205**, 3 (2002).
[24] B. Lezzar, Ph.D. thesis, Constantine, 2004.
[25] O. Hardouin Duparc, A. Larère, B. Lezzar, O. Khalfallah, and V. Paidar, J. Mater. Sci. **40**, 3169 (2005).
[26] M. Hansen, *The Constitution of Binary Alloys*, 2nd ed. (McGraw-Hill, New York, 1958).
[27] F. Ducastelle, J. Phys. (Paris) **31**, 1055 (1970).
[28] V. Rosato, M. Guillopé, and B. Legrand, Philos. Mag. A **59**, 321 (1989).
[29] M. S. S. Brooks and B. Johansson, J. Phys. F: Met. Phys. **13**, L197 (1983).
[30] M. Guillopé and B. Legrand, Surf. Sci. **215**, 577 (1989).
[31] C. H. Bennett, in *Diffusion in Solids, Recent Developments*, edited by A. S. Nowick and J. J. Burton (Academic, New York, 1975), p. 73.
[32] C. Kittel, *Introduction to Solid State Physics*, 7th ed. (Wiley, New York, 1995).
[33] G. Simmons and H. Wang, *Single Crystal Elastic Constants and Calculated Aggregates Properties* (MIT, Cambridge, MA, 1971).
[34] F. Ducastelle, *Order and Phase Stability in Alloys* (North-Holland, Amsterdam, 1991).
[35] A. V. Ruban and H. L. Skriver, Comput. Mater. Sci. **15**, 119 (1999).
[36] I. Meunier, G. Tréglia, and B. Legrand, Surf. Sci. **441**, 225 (1999).
[37] J. Friedel, Adv. Phys. **3**, 446 (1954).
[38] G. Tréglia and B. Legrand, Phys. Rev. B **35**, 4338 (1987).
[39] I. Braems, J. Creuze, F. Berthier, R. Tétot, and B. Legrand, Surf. Sci. **602**, 1903 (2008).
[40] B. Legrand, M. Guillopé, J. S. Luo, and G. Tréglia, Vacuum **41**, 311 (1990).
[41] D. J. O'Connor, H. J. Kang, P. Pigram, R. H. Roberts, and S. He, Appl. Surf. Sci. **70-71**, 114 (1993).
[42] A. Atrei, L. Pedocchi, U. Bardi, G. Rovida, M. Torrini, E. Zanazzi, M. A. van Hove, and P. N. Ross, Surf. Sci. **261**, 64 (1992).
[43] W. Chen, J. Paul, A. Barbieri, M. A. van Hove, S. Cameron, and D. J. Dwyer, J. Phys.: Condens. Matter **5**, 4585 (1993).